The Integrated-Filter Push-Pull Forward Converter for 48V Input Voltage Regulator Modules

Peng Xu, Mao Ye, Xiaochuan Jia, Pitleong Wong and Fred C. Lee

Center for Power Electronics Systems
The Bradley Department of Electrical and Computer Engineering
Virginia Polytechnic Institute and State University
Blacksburg, VA 24061 USA

***Abstract*- For high power server type of applications, the microprocessor would be driven by a voltage regulator module (VRM) that takes 48-volt input. A topology named push-pull forward converter was proposed for 48V VRM and has been proven to have a high efficiency and a fast transient response. This paper proposed an improved push-pull forward converter with an integrated magnetic. This topology is essentially a modified push-pull converter with two clamp capacitors and a coupled-inductor version of current doubler on the secondary side. We can clamp the voltage spike and recover the leakage energy. This topology also provides a built-in input filter, thus, a smooth input current. All the magnetic components are integrated in a single core. Experimental results of a 48V-to-1.2V/70A VRM prototype are given.**

I. INTRODUCTION

The advances in microprocessor technologies impose a new challenge for delivering high-quality power to these devices. With the increases of both the speed and the total transistor number within the chip, the microprocessors operate at significantly lower voltages, higher currents, and higher slew rates than before. To deliver a highly accurate supply voltage to the microprocessor, a dedicated dc/dc converter, a voltage regulator module (VRM), has to be developed and physically located next to the microprocessor. Generally, the VRM is required to have a fast transient response and a high power density.

The synchronous buck topology is widely used for the present VRMs. The interleaving technique is employed to minimize the output and decoupling capacitances and to improve the transient response. With the small output inductance, a multi-channel interleaved quasi-square-wave (QSW) VRM can further improve the transient response and increase power density.

The future generation of microprocessors will operate above 1GHz, with a further reduction of logic voltage to less than 1V and a significant increase in current consumption up to 100A. As the power demand for microprocessors increases steadily, the VRMs are required to work with a higher input voltage in order to reduce power distribution loss and simplify power deliver system design. It is the industry trend that for desktop and workstation applications, the VRM is converting 12V input to 1V output; and that the 48V VRM will emerge as a standard for server applications [6][7].

This higher input voltage requirement poses a new challenge for the VRM design. The topologies based on the synchronous buck converter may not work properly and efficiently for a large step-down power conversion such as from 12V or 48V to less than 1V.

Generally, topologies with a step-down transformer have to be used for power conversion with a large step-down ratio such as from 48V to 1.2V. The push-pull, symmetrical half-bridge, and full-bridge are the primary-side topologies suitable for this application [8].

A topology called the push-pull forward was proposed for 48V VRM in an earlier paper [9]. It has an improved transient response, reduced profile, and increased package density.

This paper proposed an improved push-pull forward converter with a single EI or EE core for all the magnetic components of the input inductor, the step-down transformer and the output inductors. The transformer's primary and secondary windings, as well as the inductor windings, are wound on the two outer legs. The leakage inductance of transformer is utilized for the input filter. Only the center leg has an air gap. The flux ripple is cancelled at the center leg, thus increasing the efficiency.

This topology is essentially a modified push-pull converter with a clamping circuit and a coupled-inductor version of current-doubler rectifier. We can clamp the voltage spike and recover the leakage energy. Due to the coupled output inductors, the inductor current ripple is greatly reduced, thus increasing the efficiency. This topology also provides a built-in input filter with a smooth input current. The built-in input filter is formed by the leakage inductance between the transformer's primary windings and the clamping capacitors. Because of a near ripple-free input current, the improved push-pull forward converter appears a higher efficiency than the original push-pull forward converter.

Section II introduces the push-pull forward converter with a current-doubler rectifier; Section III reviews the magnetic integration for the current-doubler rectifier; Section IV introduces an improved integrated magnetics for the current-doubler rectifier; Section V proposed an improved push-pull forward converter; Section VI provides the design of 48-V VRM and experiment results.

This work was supported by Delta Electronics, Hipro, Hitachi, IBM, Intel, Intersil, National Semiconductors, Power-One, TDK and Texas Instruments.

This work made use of ERC Shared Facilities supported by the National Science Foundation under Award Number EEC-9731677.

II. Push-Pull Forward VRM

Fig. 1 shows the push-pull forward converter. It has an improved transient response, reduced profile, and increased package density. This topology is essentially a modified push-pull converter topology with a clamp capacitor. One can clamp the voltage overshoot and recover the leakage energy. This topology also provides a reduced input current ripple and requires a smaller input filter.

For low-voltage, high-current applications, the secondary-side power losses have a major impact on the conversion efficiency. The synchronous rectifier is widely used to dramatically reduce the secondary-side rectification loss. The secondary-side losses can be reduced further by the proper selection of secondary-side topologies. The current-doubler topology [10][11][12] is the most popular one for high-current applications. Because of its simpler transformer secondary winding and two times lower inductor currents and transformer secondary currents, the current-doubler topology exhibits lower conduction losses than the conventional center-tapped topology.

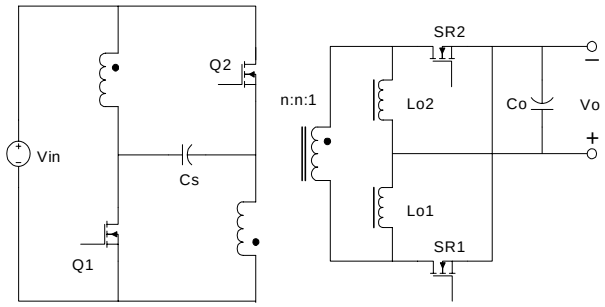

Fig. 1. Push-pull forward VRM with current-doubler rectifier.

Besides the efficiency, the transient response is another major concern for VRMs. For low voltage, high-current VRM applications, the topologies must possess a fast transient response to achieve an accurate output regulation when microprocessors operate from sleep mode to active mode and vice versa. The transient response can be improved by reducing the output filter inductance so that the rate of the inductor current change is maximized during the transient process. Due to the ripple cancellation in the current-doubler rectifier, the large ripple currents of both inductors partially cancel each other in the output current.

In summary, the push-pull forward topology with the current doubler and synchronous rectifiers is a suitable approach for high-input VRM applications.

III. Review of Magnetic Integration for Current-Doubler Rectifier

The transformer and the filter inductors in the current-doubler rectifier can be integrated into a single magnetic core. By doing so, it is possible to further improve the efficiency, while simultaneously cutting the size and cost. Fig. 2 shows the current-doubler rectifier and its discrete and integrated magnetic implementations.

Fig. 2(a) shows the schematic of the current-doubler rectifier. To simplify the following discussion, only one primary winding is drawn. The same discussion can be applied to the case with two or more primary windings, such as in push-pull topologies.

Fig. 2(b) shows the discrete magnetic implementation for the current-doubler rectifier. Three pieces of magnetic core are needed with three high-current windings and five high-current interconnections.

Fig. 2(c) shows the integrated magnetics structure proposed by O. Seiersen [10]. A single conventional EE or EI core is used with air gaps in the outer legs only. The implementation may reduce the overall size of the magnetics, since the transformer and two inductors share the outer legs of the core. It is noted that this magnetic integration focuses only on core integration while neglecting the winding integration. Three high-current windings and five high-current interconnections are still needed.

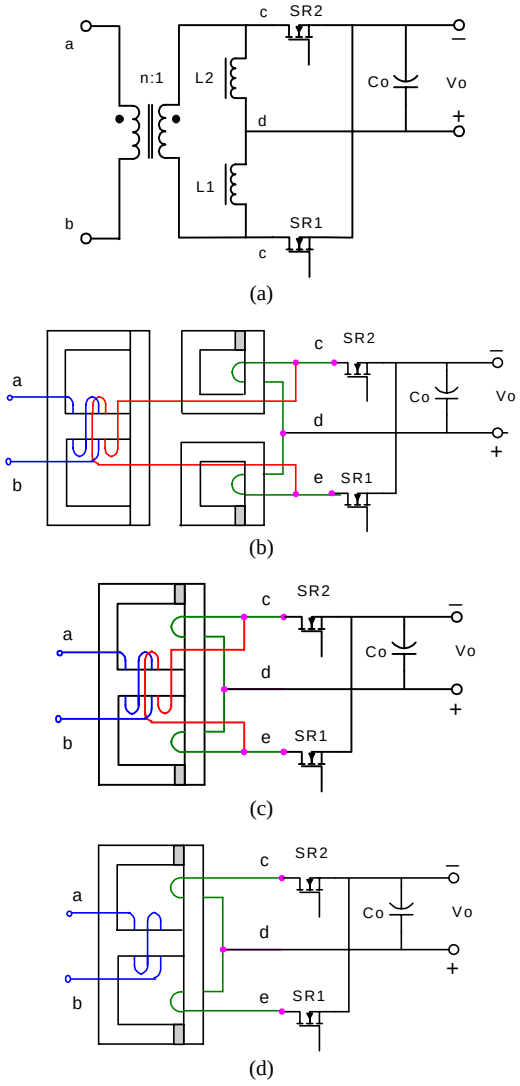

Fig. 2. (a) Current-doubler rectifier; (b) discrete magnetic implementation; (c) Seiersen's integrated magnetics, and (d) fully integrated magnetics.

Fig. 2(d) shows an improved integrated magnetics structure with a simpler winding layout [13]. Both core and winding integration are realized in this design. Not only do the transformer and two inductors share outer legs of the core, but the transformer secondary winding and inductor windings are also integrated together. Only two high-current windings and three high-current interconnections are needed. For high-current applications, this winding integration is becoming more important because of lower interconnection loss and lower conduction loss. As a result, this fully integrated magnetics structure allows for lower overall system cost and size, and higher efficiency.

All the integrated magnetics techniques discussed in this section require an EE or EI core with air gaps in the outer legs. The air gap in the center leg should be avoided, as it causes the output-inductor ripple current to increase, thus reducing the efficiency [13].

However, to ease the manufacturing, it is more desirable to have the air gap in the center leg instead of in the outer legs for a number of reasons: first, standard EE or EI cores can be used without requiring any particular gapping process; second, less electromagnetic interference (EMI) is exhibited than in the case with air gaps in outer legs; and finally, this structure ensures the mechanical stability of the core.

The air gap in the center leg introduces coupling between the two output filter inductors. Generally, this coupling is not desirable. However, by properly designing the coupling between the two inductors, both the steady-state and dynamic performances can be improved [14]. The coupled inductor concept has also been implemented into the current-doubler rectifier [15]. However, the implementation requires tow magnetic components: one for the transformer and the other for the two-coupled inductors. So far, for the coupled-inductor current-doubler rectifier, no integrated magnetics implementation has been reported.

IV. An Novel Integrated Magnetics for Coupled-Inductor Current-Doubler Rectifier

A novel integrated magnetics structure, shown in Fig. 3, is proposed for the current-doubler rectifier with two coupled inductors. It has a structure similar to one presented in an earlier paper by the authors [16]. However, in that case, the focus was on the asymmetrical half-bridge design for high-power application, and the gap design was totally different.

In the proposed structure, the primary and secondary transformer windings, as well as the inductor windings, are wound on the two outer legs. Only the center leg has an air gap.

A. Derivation of Integrated Magnetics

Fig. 4 shows the key steps to deriving the integrated magnetics structure for the current-doubler rectifier with coupled inductors. The discussion begins with the integrated magnetics structure shown in Fig. 2(d), which is called “the original structure” in this paper.

First, the primary winding is split to two outer legs so that both primary and secondary windings are wound on the same legs. Thus, the winding interleaving technique can be used to minimize the leakage inductance.

Second, the polarity of one set of windings is changed through different winding connections, as shown in step 2 of Fig. 4.

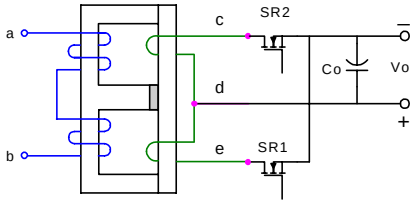

Fig. 3. Integrated magnetics for coupled-inductor current-doubler rectifier.

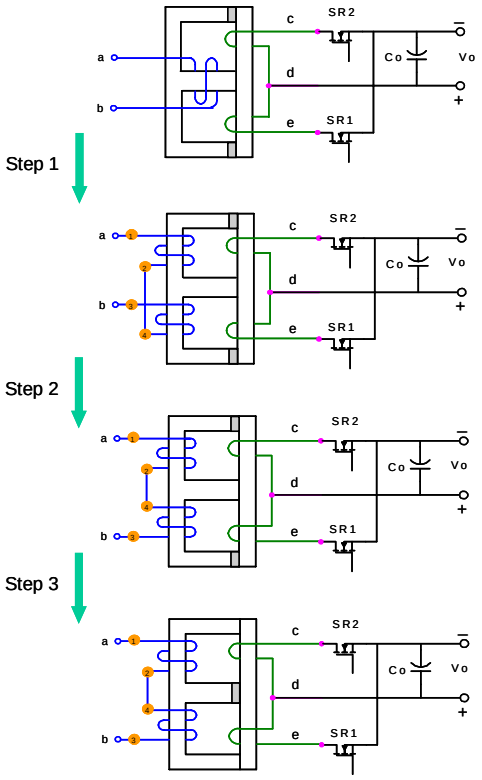

Fig. 4. Key steps to deriving integrated magnetics for the coupled-inductor current-doubler rectifier.

Finally, as shown in step 3 of Fig. 4, the air gaps in the outer legs are shifted to the center leg, and a new integrated magnetics structure is obtained.

B. Electrical Circuit Model

Fig. 5 shows the reluctance model for the proposed magnetic circuit. Ro and Rc represent the reluctance of the outer leg and the center leg, respectively. The current directions are defined according to device conduction states. The major flux directions are determined by using Right-Hand Rule, and the leakage flux paths are not considered.

The electrical circuit model can be derived from the reluctance model by use of the principle of duality [17]. Fig. 6 shows the electrical circuit model for the proposed magnetic circuit. It is the current-doubler rectifier with two coupled inductors, L1 and L2.

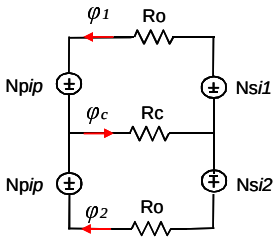

Fig. 5. Reluctance model of integrated magnetics for coupled-inductor current-doubler rectifer.

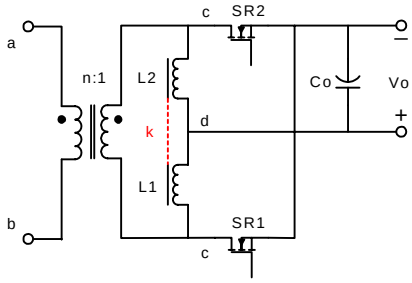

Fig. 6. Electrical model of integrated magnetics for coupled-inductor current-doubler rectifer.

The analytical relationship between the parameters of the reluctance model and the electrical model can be expressed as follows.

$$(1)\quad \begin{cases} L1 = L2 = Lo + Lm = \dfrac{(Ro + Rc)\cdot Ns^2}{Ro\cdot(Ro + 2\cdot Rc)} \\ K = \dfrac{1}{1 + \dfrac{Ro}{Rc}} \end{cases},$$

where Lo and Lm are the leakage inductance and mutual inductance of the two coupled inductors L1 and L2, respectively, and k is the coupling coefficient.

With the air gap in the center leg only, and considering the reluctance only from the air gap, then Ro<<Rc, and the coupling coefficient k approaches 1. In practice, the reluctance components from the magnetic paths can influence the value of Ro and Rc, and the typical coupling coefficient k is in the range of 0.8 to 0.9.

C. Features and Characteristics

1. Effect of Coupled Inductors

The coupling coefficient k has quite a strong influence on the current waveforms of the two coupled inductors. Fig. 7 shows the inductor and output current waveforms for different coupling coefficient k.

The coupling coefficient k influences the inductor current waveforms iL1 and iL2, but does not affect the output current io. Equation (2) shows the formula for the output current ripple. It is related only to the leakage inductance of the two coupled inductors.

$$(2)\quad \begin{cases} \Delta io = \dfrac{2\cdot Vo}{Lo\cdot fs}\cdot(1-D) \\ Lo = \dfrac{Ns^2}{Ro + 2\cdot Rc} \end{cases}$$

The larger the coupling coefficient k, the lower inductor current ripples. Since the primary and secondary device currents are reflected to the inductor currents in certain ways, coupling two output inductors can reduce the device current ripple. Thus, the conduction and switching losses can be reduced, and the overall efficiency can be improved.

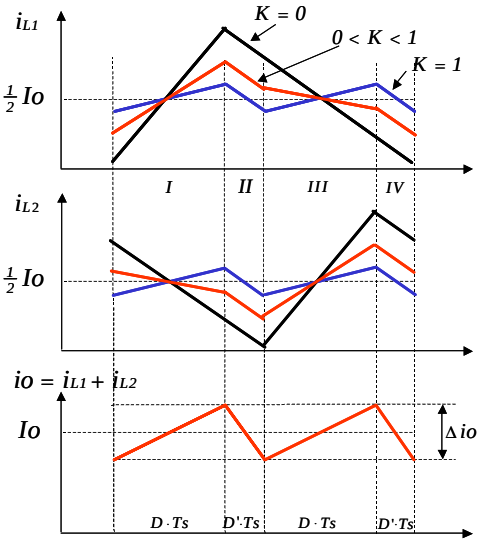

Fig. 7. Effect of coupling coefficient on current waveforms.

2. Flux Ripple Cancellation

In the proposed magnetic structure, the flux ripple at the center leg is reduced. Fig. 8 shows the flux distributions for the center leg and outer legs. As a benchmark, Fig. 8 also shows the flux distributions of Fig. 2(d)'s integrated magnetics. That is the original structure, from which the proposed structure is derived.

Fig. 9 shows the flux ripple reduction in the center leg. The original structure has a constant flux ripple, while the flux ripple reduction of the proposed structure is dependent on the duty cycle. Since the operation duty cycle is often designed close to 0.5 to maximize the efficiency, the proposed structure has a much lower flux ripple at the center leg and consequently, lower core less and higher efficiency.

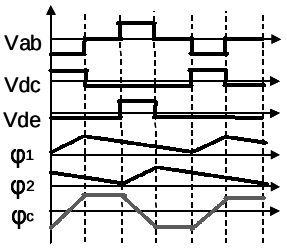

(a)

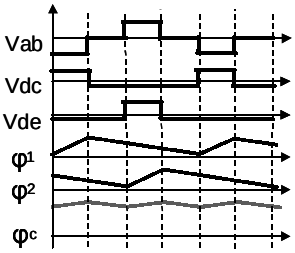

(b)

Fig. 7. Flux distribution comparison: (a) in the original structure; and (b) in the proposed structure.

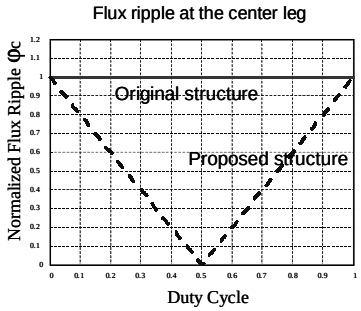

Fig. 9. Flux ripple at the center leg of the magnetic core.

3. Minimized Leakage Inductance

As shown in Fig 2(d), in the original integrated magnetics structure, the transfomer primary windings are wound on the center leg, while the secondary windings are wound on the outer legs. The coupling between the transformer primary and secondary windings is poor. A large leakage inductance is exhibited in this structure.

In the proposed structure, shown in Fig. 3, both the primary and secondary windings are wound on the outer legs. The interleaving techniques can be used to minimnize the leakage inductance of the transformer.

4. Air Gap at Center Leg Only

As previously discussed, an air gap in the center leg should be avoided in the original structure. In the proposed structure, however, the air gap can be placed in the center leg. Therefore, standard EE or EI cores can be used without requiring any particular gapping process. Less EMI is exhibited than in the case with air gaps at outer legs. This structure ensures the mechanical stability of the core. Fig. 9 shows the desirable gapping for the two structures.

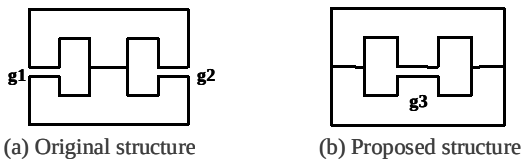

(a) Original structure (b) Proposed structure

Fig. 10. Desirable gapping: (a) original structure; and (b) proposed structure.

D. Experiment and Results

Two integrated magnetics were tested in a 48V-input, 1.2V/70A-output VRM prototype, using the push-pull forward converter. One is the original structure, and the other is the proposed structure with coupled inductors.

The prototype operates at 100kHz. The following major components of the VRM power stage were selected: primary switch – PSMN035-150B (150v, 35mohm); secondary switch – 2xSTV160NF03L (30V, 3mohm); and output inductance – 320nH.

Fig. 11 shows the design for these two integrated magnetics. The magnetic core is a combination of E32-3F3 and PLT32-3F3. The windings are made in a seven-layers 2oz P. C. board. Two primary windings have eight turns each with four turns per layer. The secondary windings use a single turn with three layers paralleled.

For the original structure, each of outer legs has a 10mil air gap, and no air gap at the center leg. The primary windings are wound on the center leg. For the proposed structure, only the center leg has a 10mil air gap. The primary windings are wound on the outer legs.

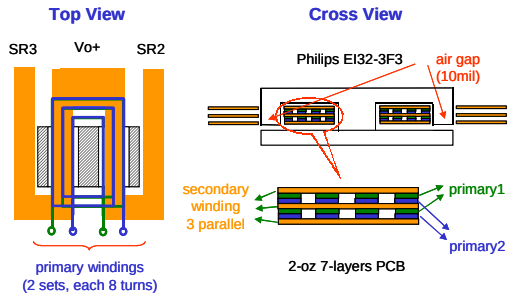

(a)

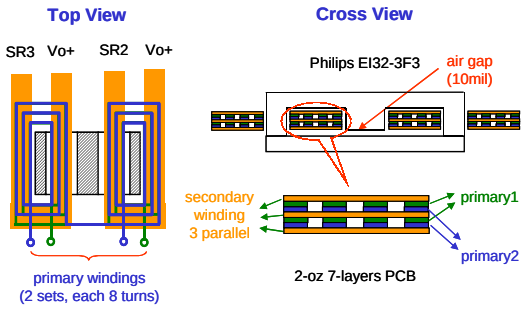

(b)

Fig. 11. Integrated magnetics design: (a) original structure, and (b) proposed structure.

The leakage inductances reflected to the secondary side were measured for both structures. The proposed structure has only 15nH leakage inductance, while the original one has 60nH. By using the proposed structure, the leakage inductance was reduced by three times.

Fig. 12 shows the key experimental waveforms at full load. By using the proposed structure, the parasitic ringing is significantly reduced, as is the primary current ripple.

Fig. 13 shows the efficiency comparison for the VRM prototype using two different integrated magnetics. By using the proposed structure, the resulting VRM has more than 83% efficiency at full load, which is 3% higher than that achieved using the original structure.

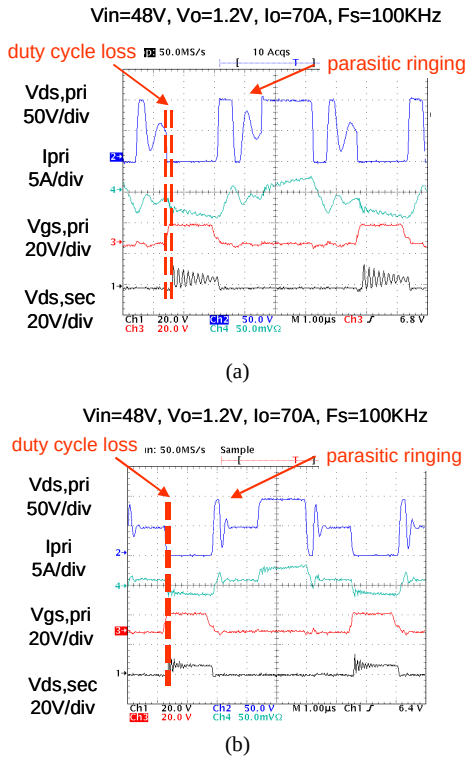

Fig. 12. Experimental waveforms at full load, (a) with original structure, (b) with proposed structure.

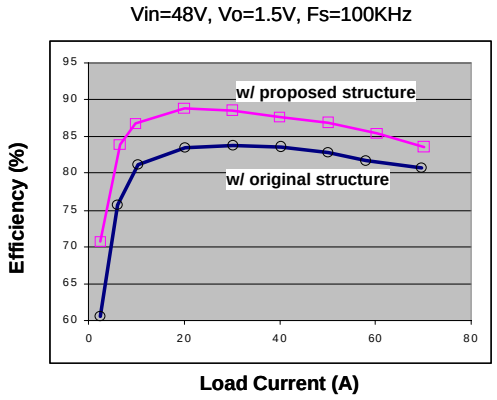

Fig. 13. VRM efficiency comparison using two integrated magnetics.

V. Improved Active-Clamp Coupled-Buck Converter with Integrated Filter

Fig.14 shows the schematic of the push-pull forward converter with the proposed integrated magnetics. Fig. 15 shows its equivalent circuits. Two circuits shown in Fig. 15 are exchangeable. Fig. 15(b)'s circuit is used for the following discussion, since the split transformer windings are shown in this circuit, which corresponding to the physical implementations shown in Fig. 14.

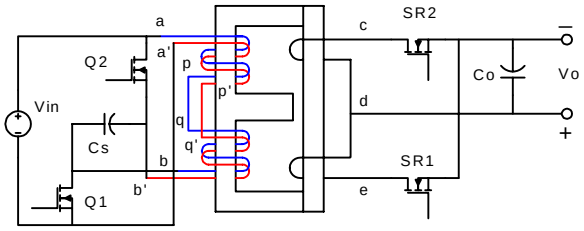

Fig. 14. Schematic for the push-pull forward converter with proposed integrated magnetics.

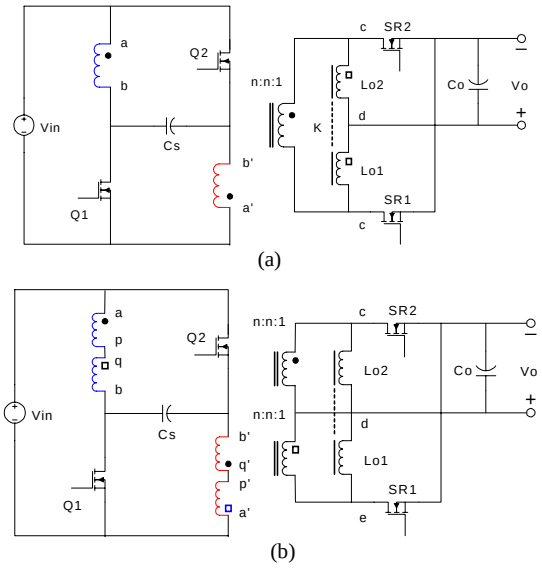

Fig. 15. Equivalent circuits of Fig. 15's implementation: (a) without showing split transformer windings; and (b) with showing split transformer windings.

Based on the equivalent circuit shown in Fig. 15(a), an improved push-pull forward converter is proposed as shown in Fig. 16. The same integrated magnetics structure is used in the improved push-pull forward converter as that in the original one. The operation principles are also same for both converters.

Fig. 17 shows the key operation waveforms for the original and improved push-pull forward converters. The operation waveforms for both converters are same except the input current. In the improved push-pull forward converter, the input current is near ripple free, while the original converter exhibits a pulsing input current.

The smooth input current means that there is a built-in input filter existing in the improved push-pull forward converter. The built-in input filter is formed by the leakage inductance and the clamping capacitor. Actually, the concept for the built-in filter here is same as one in other topologies described in earlier papers [18][19].

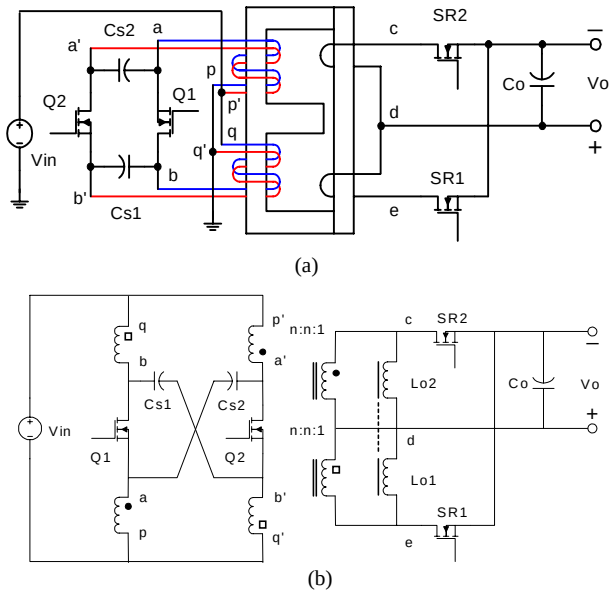

Fig. 16. Improved push-pull forward converter: (a) schematic; and (b) equivalent circuit.

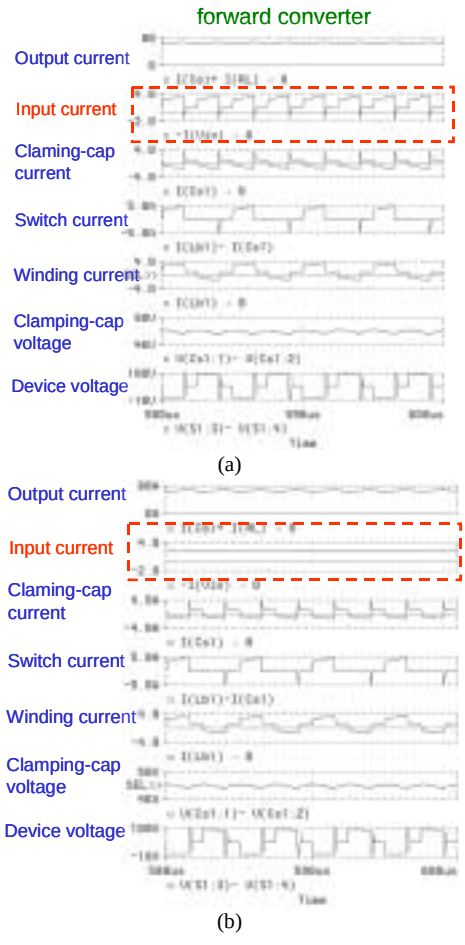

Fig. 17 Key operation waveforms of push-pull forward converters: (a) original version, and (b) improved version.

Because of the built-in input filter, the input filter size of the improved push-pull forward converter would be reduced, and sometimes even no external input filter is needed. Fig. 18 shows an implementation without requiring an external input filter. The suitable leakage inductance of the transformer windings is utilized as the input filter inductor, while the clamping capacitors are serving as the filter capacitors.

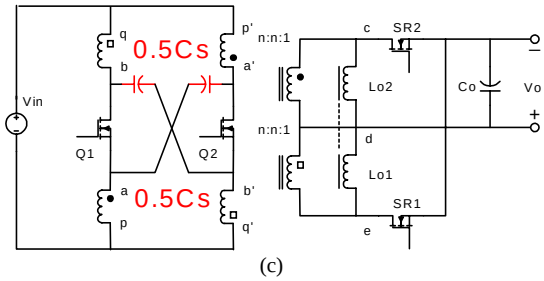

Fig. 18. Improved push-pull forward converter with fully integrated filter.

VI. Experiments and Results

Three 48V-input, 1.2V/70A-output VRM prototypes were built. The prototypes operate at 100kHz. One prototype uses the conventional push-pull topology, and the other two use the original version and the improved version of the push-pull forward converter, respectively.

Three prototypes have the same major components for the power stage: primary switch – PSMN035-150B (150v, 35mohm); secondary switch – 2xSTV160NF03L (30V, 3mohm); and output inductance – 320nH. Three prototypes are using the identical integrated magetics and the secondary sides. The integrated magnetics structure is shown in Fig. 11(b). The magnetic core is a combination of E32-3F3 and PLT32-3F3. Two primary windings have eight turns each with four turns per layer. The secondary windings use a single turn with three layers paralleled. Only the center leg has a 10mil air gap.

The leakage inductance measured at the primary side is about 1.4 uH. The clamping capacitor for the push-pull forward converter is 2x3.3uF. In the conventional push-pull forward converter, an additional R-C snubber (100ohm-750pF) is employed to control the device voltage spike caused by the leakage energy.

Fig. 19 shows their experimental waveforms at full load. The conventional push-pull converter has a pulsing current. The original push-pull forward converter has a reduced input RMS current, however, the input current is still pulsing with a DC-current bias. In the improved push-pull forward converter, the input current is smooth.

Fig. 20 shows the efficiency comparison. Both two push-pull forward converters have more than 3% higher efficiency than the conventional push-pull forward converter. The improved push-pull forward converter appears the highest efficiency among three, with a 91% ceiling efficiency and an 85% full-load efficiency.

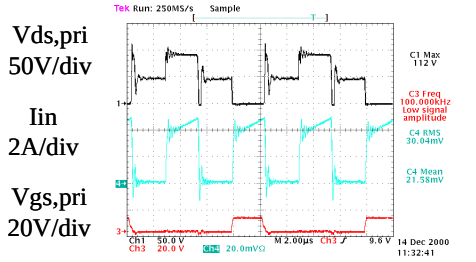

Push-Pull

(a)

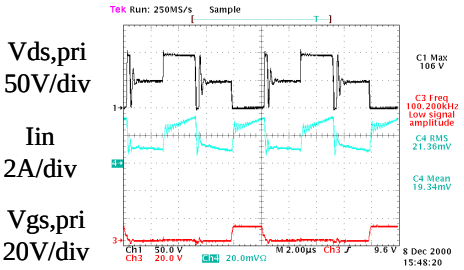

Push-Pull Forward

(b)

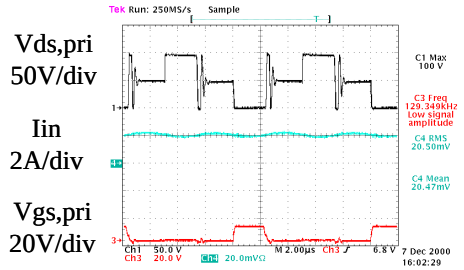

Integrated-Filter Push-pull Forward

(c)

Fig. 19. Experimental waveforms at full load: (a) conventional push-pull, (b) original push-pull forward: and (c) improved push-pull forward.

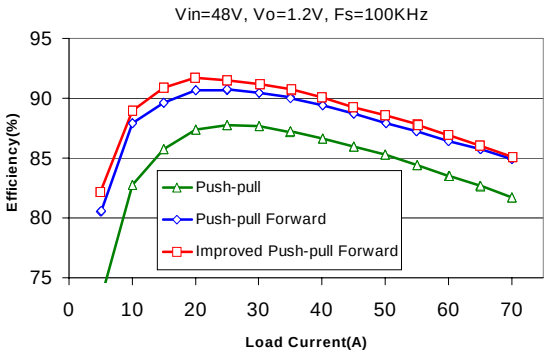

Fig. 20. Measured VRM efficiency.

V. SUMMARY

The push-pull forward with synchronous rectifier and current-doubler rectifier is a suitable scheme for high-input VRM design. In the push-pull forward topology, an integrated magnetics structure has been proposed for the current-doubler rectifier in order to make the high-input VRM more efficient, more compact and less expensive, where the transformer's primary and secondary windings, as well as the inductor windings, are wound on the two outer legs. An improved push-pull forward converter has been proposed further by utilizing the leakage inductance of the integrated magnetics and the clamping capacitors for the input filter. With the built-in input filter, we can reduce the size and improve the efficiency further.

REFERENCES

[1] Michael T. Zhang, Milan M. Jovanovic and Fred C. Lee, "Design Consign Considerations for Low-Voltage On-board DC/DC Modules for Next Generations of Data Processing Circuits," IEEE Transactions on Power Electronics, Vol. 11, No. 2, March 1996.

[2] Xunwei Zhou, Xingzhu Zhang, Jiangang Liu, Pit-Leong Wong, Jiabin Chen, Ho-Pu Wu, Luca Amoroso, Fred C. Lee, and Dan Y. Chen, " Investigation of Candidate VRM Topologies for future Microprocessors," IEEE APEC'98.

[3] Y. Panvo and M.M. Jovanovic, "Design Consideration for 12V/1.5V, 50A Voltage Regulator Modules," IEEE APEC'2000

[4] P. Xu, X. Zhou, P.L Wong, K. Yao and F.C. Lee, "Design and Performance Evaluation of Multi-Channel Interleaving Quasi-Square-Ware Buck Voltage Regulator Module," HFPC'2000.

[5] Xunwei Zhou, Peng Xu, and Fred C. Lee "A High Power Density, High Frequency and Fast Transient Voltage Regulator Module wit a Novel Current Sharing and Current Sharing Technique," IEEE APEC'99.

[6] Intel Corp., "VRM 9.0 DC-DC Converter Design Guidelines", Nov. 2000.

[7] Intel Corp., "Server Distributed Power 48 V Input (Advanced) DC-to-DC Converter Design Specification".

[8] Y. Panvo and M. M. Jovanovic, "Design and Performance Evaluation of Low-Voltage/High-Current DC/DC On-Board Modules," IEEE APEC'99

[9] Xunwei Zhou, Bo Yang, Luca Amoroso, Fred C. Lee and Pit-leong Wong, "A Novel High-input-voltage, High Efficiency and Fast Transient Voltage Regulator Module: The Push-pull Forward Converter", APEC'99.

[10]C. Peng, M. Hannigan, O. Seiersen, "A new efficient high frequency rectifier circuit", *High Frequency Power Conversion Conference Proceedings*, pp. 236-243, June 1991.

[11]K. O'Meara, "A new output rectifier configuration optimized for high frequency operation", *High Frequency Power Conversion Conference Proceedings*, pp. 219-225, June 1991.

[12]L. Balogh, "The performance of the current doubler rectifier with synchronous rectification", *High Frequency Power Conversion Conference Proceedings*, pp. 216-225, May 1995.

[13]W. Chen, G. Hua, D. Sable, F. C. Lee, "Design of high efficiency, low profile, low voltage converter with integrated magnetics", *IEEE APEC'97*, pp. 911-917, 1997.

[14]Pit-Leong Wong, Qiaoqiao Wu, Peng Xu, Bo Yang and Fred C. Lee, "Investigating Coupling Inductors in the Interleaving QSW VRM," IEEE APEC 2000.

[15]A. Pietkiewicz and D. Tollik, "Coupled-Inductor Current-Doubler Topology in Phase-Shifted Full-Bridge DC-DC Converter", INTELEC'99, PP. 41-48.

[16]Peng Xu, Qiaoqiao Wu, Pitleong Wong and Fred C. Lee, "A Novel Integrated Current-Doubler Rectifier", APEC'2000.

[17]J. K. Watson, "Application of Magnetism", John Wiley & Sons, 1980.

[18]Edward Herbert, "Analysis of the Near Zero Input Current Ripple Condition in a Symmetrical Push-Pull Power Converter", HFPC'89.

[19] Ching-Shan Leu and Junn-Bin Hwang, "A Built-in Input Filter Forward Converter", PESC'94.